Beyond the Random Phase Approximation for the Electron Correlation Energy: The Importance of Single Excitations

Xinguo Ren, Alexandre Tkatchenko, Patrick Rinke, and Matthias Scheffler
Fritz-Haber-Institut der Max-Planck-Gesellschaft, Faradayweg 4-6, 14195, Berlin, Germany

The random phase approximation (RPA) for the electron correlation energy, combined with the exact-exchange energy, represents the state-of-the-art exchange-correlation functional within density-functional theory (DFT). However, the standard RPA practice – evaluating both the exact-exchange and the RPA correlation energy using local or semilocal Kohn-Sham (KS) orbitals – leads to a systematic underbinding of molecules and solids. Here we demonstrate that this behavior is largely corrected by adding a "single excitation" (SE) contribution, so far not included in the standard RPA scheme. A similar improvement can also be achieved by replacing the non-self-consistent exact-exchange total energy by the corresponding self-consistent Hartree-Fock total energy, while retaining the RPA correlation energy evaluated using Kohn-Sham orbitals. Both schemes achieve chemical accuracy for a standard benchmark set of non-covalent intermolecular interactions.

In the quest for finding an "optimal" electronic structure method, that combines accuracy and tractability with transferability across different chemical environments and dimensionalities (e.g. molecules, wires/tubes, surfaces, solids), the treatment of exchange and correlation in terms of "exact-exchange plus correlation in the random-phase approximation (EX+cRPA)" [1, 2] offers a promising avenue [3–18]. In this approach, part of the exact-exchange (EX) energy cancels exactly the spurious self-interaction error present in the Hartree energy. And the RPA correlation (cRPA) energy is fully non-local, whereby long-range van der Waals (vdW) interactions are included automatically and accurately [19]). Morever, dynamical electronic screening is taken into account by summing up a sequence of "ring" diagrams to infinite order, making EX+cRPA applicable to small-gap or metallic systems where, for example, Hartree-Fock (HF) plus 2nd-order Møller-Plesset (MP2) perturbation theory [20] breaks down.

The concept of cRPA dates back to the many-body treatment of the uniform electron gas in the 1950s [1, 2], and was later formulated within the context of density-functional theory (DFT) [21] via the adiabatic-connection fluctuation-dissipation theorem [22]. Recent years have witnessed a revived interest in EX+cRPA and its variants in quantum chemistry [3–9, 23], solid state physics [10–13], and surface science [14–17]. Within the framework of Kohn-Sham (KS) DFT, EX+cRPA embodies an orbital-dependent functional that can in principle be solved self-consistently via the optimized effective potential (OEP) approach [24]. Exploiting this variational principle of the energy functional, practical EX+cRPA calculations are commonly performed in a post-processing fashion, where eigenvalues and orbitals from a self-consistent DFT calculation in the local-density approximation (LDA), generalized gradient approximations (GGAs), or alike, are used to evaluate both the EX and cRPA terms. Alternatively, one can formulate cRPA in terms of many-body perturbation theory (MBPT) based on a Hartree-Fock (HF) reference state.

Throughout this Letter we will adopt the following nomenclature: E^F@SC is the total energy of the functional F, evaluated with the orbitals of a self-consistent (SC) scheme, e.g., HF, or the Perdew-Burke-Ernzerhof (PBE) [25] GGA. The corresponding theoretical scheme is then labeled F@SC. We also use the letter "x" or "c" in front of F or as a subscript of E^F to refer to the exchange or correlation part of the scheme explicitly. The functional F can be exact exchange (EX), or additionally contain RPA correlation (EX+cRPA), etc. For example, E^{EX}@HF is the self-consistent Hartree-Fock energy, whereas the conventional RPA scheme based on PBE orbitals is referred to as (EX+cRPA)@PBE.

The original schemes (EX+cRPA)@HF and (EX+cRPA)@PBE both exhibit systematic underbinding for different types of systems, including covalent molecules [3], weakly bonded molecules [7, 8], solids [11, 12], and molecules adsorbed on surfaces [15, 16, 26]. Several attempts have been made to improve the accuracy of EX+cRPA. The earliest is the so-called RPA+ scheme [27] where a local correction at the LDA/GGA level is added to cRPA. More recent attempts add second-order screened exchange (SOSEX) [9, 28]) to make the entire approach self-correlation free, or invoke cRPA in a range-separated framework where only the long-range part of cRPA is incorporated [7, 8] Among these, RPA+ improves total correlation energies considerably [29], but not binding energies [3]. The SOSEX correction performs well [9, 28] with considerable additional numerical effort. Range-separated RPA schemes also improve upon the standard EX+cRPA scheme [7, 8, 18], however, at the price of introducing empirical parameters in the approach.

In this Letter, we offer a new perspective for going beyond cRPA, and show that a simple modification of the standard EX+cRPA scheme leads to a signifi-

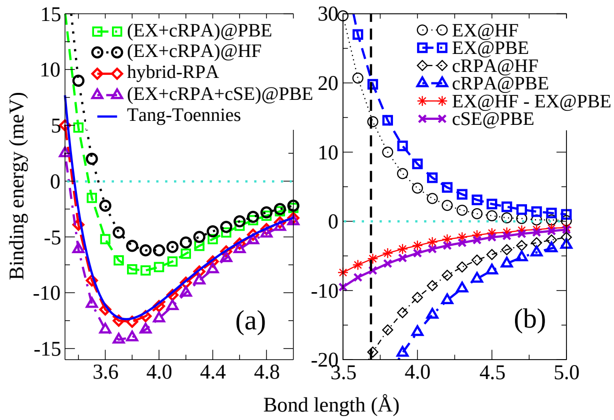

FIG. 1: (Color online) Panel (a): Binding energy curve for Ar_2 computed with four RPA-based approaches, in comparison to the accurate reference curve by Tang and Toennies [30]. Panel (b): Decomposition of the $E^{\mathrm{EX+cRPA}}$@HF ($E^{\mathrm{EX+cRPA}}$@PBE) binding energy of Ar_2 into individual contributions: E^{EX}@HF (E^{EX}@PBE) and $E_{\mathrm{c}}^{\mathrm{RPA}}$@HF ($E_{\mathrm{c}}^{\mathrm{RPA}}$@PBE). The difference between E^{EX}@HF and E^{EX}@PBE, and the $E_{\mathrm{c}}^{\mathrm{SE}}$ term are also plotted. The vertical dashed line marks the equilibrium distance. Calculations are done with FHI-aims [31, 32] and Dunning's aug-cc-pV6Z basis [33]. The basis set superposition error (BSSE) is corrected using the counterpoise scheme here and in the following.

cant accuracy increase for molecular binding energies. We first illustrate our essential idea using the example of Ar_2. The (EX+cRPA)@PBE and (EX+cRPA)@HF binding energy curves for Ar_2 are plotted in Fig. 1(a). Both schemes show a significant underbinding behavior compared to the reference curve modeled by Tang and Toennies [30] based on experimental data. To gain more insight into the origin of the underbinding, the EX+cRPA binding energies are decomposed into two contributions in Fig. 1(b): exact-exchange and the remaining cRPA part. An inspection of the individual components reveals that $E_{\mathrm{c}}^{\mathrm{cRPA}}$@HF is (much) more repulsive than $E_{\mathrm{c}}^{\mathrm{cRPA}}$@PBE, whereas at the exact-exchange level E^{EX}@PBE is (much) more repulsive than E^{EX}@HF. The fact that $E_{\mathrm{c}}^{\mathrm{cRPA}}$@PBE is more attractive than $E_{\mathrm{c}}^{\mathrm{cRPA}}$@HF is easy to rationalize by inspecting the frequency-dependent polarizabilities. Extensive benchmark calculations for 1225 molecular pairs [34] show that asymptotic C_6 dispersion coefficients derived from $E_{\mathrm{c}}^{\mathrm{cRPA}}$@HF are systematically too small by approximately 40% [32], while this error is only $\sim$ 10% for $E_{\mathrm{c}}^{\mathrm{cRPA}}$@PBE. Adding ΔvdW corrections in an attempt to reduce the remaining error in cRPA@PBE [35] only leads to minor changes in the binding energy at the equilibrium distance. What is more striking, however, is the considerable difference in binding energies at the exact-exchange level, E^{HF}@HF$-E^{\mathrm{EX}}$@PBE (plotted also in Fig. 1(b) (red stars)). It amounts to $\sim$6 meV at the equilibrium distance and is thus close to the deviation of the EX+cRPA@PBE binding energy from the reference value.

From the viewpoint of MBPT, E^{EX}@HF and E^{EX}@PBE correspond to the first-order in a perturbative expansion of the respective HF or PBE reference state. The difference between E^{EX}@HF and E^{EX}@PBE must therefore be compensated by higher-order terms in the perturbation since the final result should be independent of the reference state, if all terms were summed up. The next term in the series is the 2nd-order correlation energy $E_{\mathrm{c}}^{(2)}$, the significance of which is illustrated by the fact that $2E_{\mathrm{c}}^{(2)}$ gives the initial slope in the adiabatic connection of the exact DFT correlation energy [36]. In this work we examine the contribution of single excitations (SE) to $E_{\mathrm{c}}^{(2)}$, which can be expressed [37] as

$$E_{\mathrm{c}}^{\mathrm{SE}} = \sum_{i}^{\mathrm{occ}} \sum_{a}^{\mathrm{unocc}} \frac{|\langle \psi_i | \hat{f} | \psi_a \rangle|^2}{\epsilon_i - \epsilon_a}. \tag{1}$$

Here ψ_i and ϵ_i are the single particle orbitals and orbital energies of the reference state, and $\hat{f}$ is the single-particle HF Hamiltonian – the Fock operator. A more detailed derivation of Eq. (1) is given in the supplementary material. As a consequence of the Brillouin theorem [37], $E_{\mathrm{c}}^{\mathrm{SE}}$ trivially vanishes for HF orbitals, but is in general non-zero for KS orbitals. The contribution of $E_{\mathrm{c}}^{\mathrm{SE}}$ evaluated with PBE orbitals (referred to as cSE@PBE) to the binding energy of Ar_2 is plotted in Fig. 1(b) (violet crosses). It amounts to 50% of the binding energy at the equilibrium distance and is close in magnitude to the contribution from E^{EX}@HF$-E^{\mathrm{EX}}$@PBE. It accounts almost fully for the underbinding in the original (EX+cRPA)@PBE scheme. We therefore propose the addition of $E_{\mathrm{c}}^{\mathrm{SE}}$ to $E^{\mathrm{EX+cRPA}}$ (subsequently referred to as EX+cRPA+cSE) as new scheme. The resultant (EX+cRPA+cSE)@PBE binding energy curve for Ar_2 is also plotted in Fig. 1(a). One can see that it improves considerably over the (EX+cRPA)@PBE results, and is in close agreement with the Tang-Toennies reference curve.

It appears that the quantitative agreement between $E_{\mathrm{c}}^{\mathrm{SE}}$ defined in Eq. (1) and E^{EX}@HF$-E^{\mathrm{EX}}$@PBE is a general feature. We found for a set of 50 atoms and molecules that the agreement typically ranges between 70% and 100%. This suggests that replacing E^{EX}@PBE by E^{EX}@HF is an effective way to account for the SE contributions. A "hybrid-RPA" scheme, whose total energy is given by

$$E^{\mathrm{hybrid\text{-}RPA}} = E^{\mathrm{EX}}@\mathrm{HF} + E_{\mathrm{c}}^{\mathrm{cRPA}}@\mathrm{PBE}. \tag{2}$$

is therefore an alternative to boost the accuracy of RPA. Fig. 1(a) shows that the resultant binding energy curve is in almost perfect agreement with the reference curve.

At this point, it is illustrative to take a closer look at the individual contributions to E^{EX}@HF$-E^{\mathrm{EX}}$@PBE. In

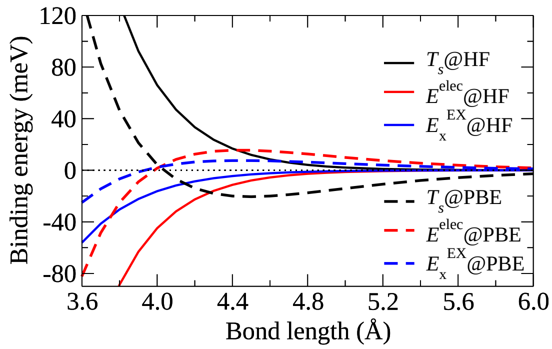

FIG. 2: (Color online) Decomposition of the E^{EX}@HF and E^{EX}@PBE binding energies for Ar_2 into their kinetic, electrostatic, and exchange components.

Fig. 2 we further decompose the EX@HF and EX@PBE binding energies into their kinetic (T_{s}), electrostatic (E^{elec}, external potential energy and Hartree energy combined), and exact-exchange components (E_x^{EX}) for Ar_2. All three energy components behave quite differently for HF and PBE orbitals. The HF kinetic energy is purely repulsive, whereas the PBE one exhibits spurious attraction at intermediate and large distances. The HF electrostatic and exact-exchange energies, on the other hand, are purely attractive and decay to zero from below, while the corresponding PBE ones become repulsive in the intermediate range and decay to zero from above at large distances. Since the PBE orbitals are less localized than their HF counterparts all three energy components decay much slower in PBE than in HF. The overall effect is that E^{EX}@PBE becomes significantly more repulsive than E^{EX}@HF, resulting in the underbinding behavior of (EX+cRPA)@PBE. This explains why the SE term, which would change the PBE orbitals if applied to the orbitals directly, corrects the unphysical behavior of the components in E^{EX}@PBE and counteracts its too-repulsive nature.

The exceptional performance of the (EX+cRPA+cSE)@PBE and hybrid-RPA schemes for rare-gas dimers carries over to many other molecular systems. Here we show results for the N_2 molecule adsorbed on benzene (N_2@benzene), which is an important model system for studying molecular adsorption on graphene and graphite surfaces [38]. We consider two possible configurations: N_2 placed parallel or perpendicular to the benzene plane. A successful theoretical approach for this system must be able to describe the delicate balance between electrostatic and dispersion interactions. We use FHI-aims' [31, 32] numeric atom-centered orbital basis ($6s5p4d3f2g$ for C, O, N, and $5s3p2d1f$ for H) [31] augmented with gaussian aug-cc-pV5Z diffuse functions to achieve convergence of the binding energy to within 1 meV. The results shown in Fig. 3 are very similar to the rare-gas dimers: (EX+cRPA)@HF and (EX+cRPA)@PBE underbind significantly at the equilibrium distance, while hybrid-RPA and (EX+cRPA+cSE)@PBE bring the binding energy into much closer agreement with the reference curve computed with the coupled cluster method including single, double and perturbative triple excitations (CCSD(T)) [38].

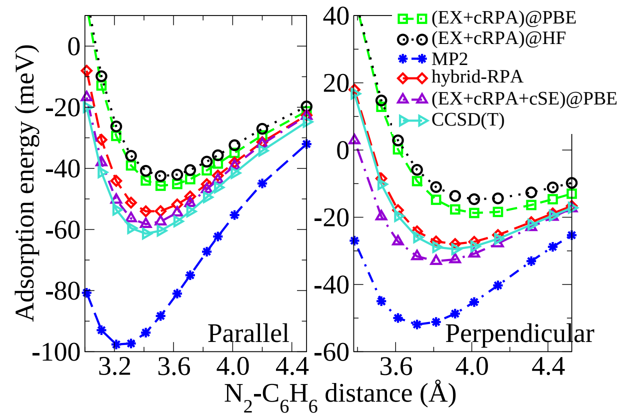

FIG. 3: (Color online) Binding energies of the parallel and perpendicular configuration of N_2@benzene as a function of the N_2-$\mathrm{C}_6\mathrm{H}_6$ center-of-mass distance, calculated by different RPA-based approaches as well as MP2 compared to reference CCSD(T) calculations from Ref. [38].

TABLE I: Mean absolute error (in meV) and mean absolute percentage error (in parenthesis) of different RPA-based approaches for the S22 database [39]. CCSD(T) extrapolated to the complete basis set limit [40] is taken as reference.

	H-bond	Dispersion	Mixed
(EX+cRPA)@HF	45 (8.5%)	70 (43.9%)	34 (20.9%)
(EX+cRPA)@PBE	57 (11.2%)	36 (21.8%)	24 (15.0%)
(EX+cRPA+cSE)@PBE	30 (6.0%)	18 (12.0%)	8 (5.5%)
hybrid-RPA	18 (3.0%)	17 (10.0%)	8 (5.1%)

Finally we examine the performance of (EX+cRPA+cSE)@PBE and hybrid-RPA for the S22 database of Jurečka *et al.* [39], which represents a balanced benchmark set for non-covalent interactions. The molecular dimers in this database can be divided into three groups of different bonding types: hydrogen-bonded, dispersion-bonded, and mixed complexes. We note that RPA in a range-separated framework has been applied to the S22 database very recently [18]. In Fig. 4 we plot the deviation from the CCSD(T) reference values [40] for the binding energies in the S22 database [39] for (EX+cRPA)@HF, (EX+cRPA)@PBE, MP2, (EX+cRPA+cSE)@PBE, and hybrid-RPA. The basis set type and quality is the same as for N_2@benzene. A detailed error analysis is presented in Table I.

We observe that the standard (EX+cRPA)@PBE scheme systematically underbinds all complexes. (EX+cRPA)@HF performs even worse for dispersion and mixed bonding, but better for hydrogen bonding.

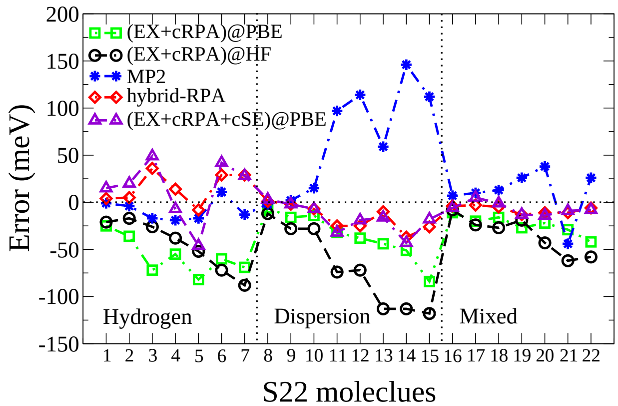

FIG. 4: (Color online) Deviation from the CCSD(T) reference values [40] for the binding energies of the S22 database [39] for RPA-based approaches as well as MP2. Positive errors correspond to overbinding and negative ones to underbinding.

The latter case can be explained by the fact that the better performance of EX@HF dominates over the bad performance of cRPA@HF for hydrogen bonded systems. Again (EX+cRPA+cSE)@PBE and hybrid-RPA correct the underbinding behavior of the standard EX+cRPA schemes, and improve the accuracy considerably. The hybrid-RPA scheme yields a mean absolute error (MAE) of 14 meV. The performance of (EX+cRPA+cSE)@PBE is very similar for dispersion and mixed bonding, albeit somewhat worse for hydrogen bonding. However, the mean absolute percentage error for hydrogen bonding (6%) is still quite small. Finally we note that atomization energies of covalent molecules are also improved considerably by (EX+cRPA+cSE)@PBE and hybrid-RPA. However, for a more detailed analysis we refer to future work [32].

To summarize, we have unraveled the origin of the underbinding in the standard (EX+cRPA)@PBE scheme, which is mainly due to the too-repulsive nature of E^{EX}@PBE rather than the underestimation of the long-range dispersion coefficients by $E_{\mathrm{c}}^{\mathrm{cRPA}}$@PBE. This problem can be largely solved either by replacing E^{EX}@PBE by the self-consistent HF energy E^{EX}@HF, or by adding a SE correction to the standard (EX+cRPA)@PBE approach. Particularly (EX+cRPA+cSE)@PBE is a well-defined parameter-free scheme in which the cSE term is much cheaper to compute than the cRPA term, and hence does not add any significant computational cost to the approach. Encouraged by its remarkable performance for weak interactions, we therefore propose the EX+cRPA+cSE scheme as a new starting point for future developments of RPA-based approaches. Moreover one can easily generalize the cSE contributions at the 2nd-order by summing up a geometrical series of higher-order diagrams involving single excitations (in the spirit of cRPA). This generalization will make EX+cRPA+cSE more robust, and allow it to be applied to systems with vanishing gaps. The details of this generalized scheme will be presented elsewhere [32]. In addition, the SE correction is compatible with other beyond-RPA schemes like RPA+ or SOSEX [41].

[1] D. Bohm and D. Pines, Phys. Rev. **92**, 609 (1953).
[2] M. Gell-Mann and K. A. Brueckner, Phys. Rev. **106**, 364 (1957).
[3] F. Furche, Phys. Rev. B **64**, 195120 (2001).
[4] M. Fuchs and X. Gonze, Phys. Rev. B **65**, 235109 (2002).
[5] F. Furche and T. Van Voorhis, J. Chem. Phys. **122**, 164106 (2005).
[6] G. E. Scuseria, T. M. Henderson, and D. C. Sorensen, J. Chem. Phys. **129**, 231101 (2008).
[7] B. G. Janesko, T. M. Henderson, and G. E. Scuseria, J. Chem. Phys. **130**, 081105 (2009).
[8] J. Toulouse *et al.*, Phys. Rev. Lett. **102**, 096404 (2009).
[9] J. Paier *et al.*, J. Chem. Phys. **132**, 094103 (2010).
[10] A. Marini, P. García-González, and A. Rubio, Phys. Rev. Lett **96**, 136404 (2006).
[11] J. Harl and G. Kresse, Phys. Rev. B **77**, 045136 (2008).
[12] J. Harl and G. Kresse, Phys. Rev. Lett. **103**, 056401 (2009).
[13] D. Lu, Y. Li, D. Rocca, and G. Galli, Phys. Rev. Lett. **102**, 206411 (2009).
[14] J. F. Dobson and J. Wang, Phys. Rev. Lett **82**, 2123 (1999).
[15] M. Rohlfing and T. Bredow, Phys. Rev. Lett **101**, 266106 (2008).
[16] X. Ren, P. Rinke, and M. Scheffler, Phys. Rev. B **80**, 045402 (2009).
[17] L. Schimka *et al.*, Nature Materials **9**, 741 (2010).
[18] W. Zhu *et al.*, J. Chem. Phys. **132**, 244108 (2010).
[19] J. F. Dobson, in *Topics in Condensed Matter Physics*, edited by M. P. Das (Nova, New York, 1994).
[20] C. Møller and M. S. Plesset, Phys. Rev. **46**, 618 (1934).
[21] W. Kohn and L. J. Sham, Phys. Rev. **140**, A1133 (1965).
[22] D. C. Langreth and J. P. Perdew, Phys. Rev. B **15**, 2884 (1977).
[23] F. Furche, J. Chem. Phys. **129**, 114105 (2008).
[24] S. Kümmel and L. Kronik, Rev. Mod. Phys. **80**, 3 (2008).
[25] J. P. Perdew, K. Burke, and M. Ernzerhof, Phys. Rev. Lett **77**, 3865 (1996).
[26] J. Harl, L. Schimka, and G. Kresse, Phys. Rev. B **81**, 115126 (2010).
[27] S. Kurth and J. P. Perdew, Phys. Rev. B **59**, 10461 (1999).
[28] A. Grüneis *et al.*, J. Chem. Phys. **131**, 154115 (2009).
[29] H. Jiang and E. Engel, J. Chem. Phys **127**, 184108 (2007).
[30] K. T. Tang and J. P. Toennies, J. Chem. Phys. **118**, 4976 (2003).
[31] V. Blum *et al.*, Comp. Phys. Comm. **180**, 2175 (2009).
[32] X. Ren *et al.*, in preparation.
[33] J. T. H. Dunning, J. Chem. Phys. **90**, 1007 (1989).
[34] A. Tkatchenko and M. Scheffler, Phys. Rev. Lett. **102**, 073005 (2009).
[35] A. Tkatchenko *et al.*, J. Chem. Phys. **131**, 094106 (2009).
[36] S. Ivanov and M. Levy, J. Phys. Chem. A **102**, 3151 (1998).

[37] A. Szabo and N. S. Ostlund, *Modern Quantum Chemistry: Introduction to Advanced Electronic Structure Theory* (McGraw-Hill, New York, 1989).

[38] A. Tkatchenko *et al.*, submitted.

[39] P. Jurečka *et al.*, Phys. Chem. Chem.Phys. **8**, 1985 (2006).

[40] T. Takatani *et al.*, J. Chem. Phys. **132**, 144104 (2010).

[41] J. Paier *et al.*, in preparation.

Derivation of the single excitation contribution to the 2nd order correlation energy

In this supplementary material we derive Eq. (1) that is presented in the main part of this Letter – the single excitation contribution to the 2nd-order correlation energy – from Rayleigh-Schrödinger perturbation theory (RSPT). The interacting N-electron system at hand is governed by the Hamiltonian

$$\hat{H} = \sum_{i=1}^{N}\left[-\frac{1}{2}\nabla_i^2 + \hat{v}_{\rm ext}(\mathbf{r}_i)\right] + \sum_{i<j}^{N}\frac{1}{|\mathbf{r}_i-\mathbf{r}_j|},$$

where $\hat{v}_{\rm ext}(\mathbf{r})$ is a local, multiplicative external potential. In RSPT, $\hat{H}$ is partitioned into a non-interacting mean-field Hamiltonian $\hat{H}^0$ and an interacting perturbation $\hat{H}'$,

$$\begin{aligned}
\hat{H} &= \hat{H}^0 + \hat{H}' \\
\hat{H}^0 &= \sum_{i=1}^{N}\hat{h}^0(i) = \sum_{i=1}^{N}\left[-\frac{1}{2}\nabla_i^2 + \hat{v}_{\rm ext}(\mathbf{r}_i) + \hat{v}_i^{\rm MF}\right] \\
\hat{H}' &= \sum_{i<j}^{N}\frac{1}{|\mathbf{r}_i-\mathbf{r}_j|} - \sum_{i=1}^{N}\hat{v}_i^{\rm MF}.
\end{aligned}$$

Here $\hat{v}^{\rm MF}$ is any mean-field potential, which can be non-local, as in the case of Hartree-Fock (HF) theory, or local, as in the case of Kohn-Sham (KS) theory.

Suppose the solution of the single-particle Hamiltonian $\hat{h}^0$ is known

$$\hat{h}^0|\psi_p\rangle = \epsilon_p|\psi_p\rangle, \tag{1}$$

then the solution of the non-interacting many-body Hamiltonian H^0 follows

$$\hat{H}^0|\Phi_n\rangle = E_n^{(0)}|\Phi_n\rangle.$$

The $|\Phi_n\rangle$ are single Slater determinants formed from N of the spin orbitals $|p\rangle = |\psi_p\rangle$ determined in Eq. (1). These Slater determinants can be distinguished according to their excitation level: the ground-state configuration $|\Phi_0\rangle$, singly excited configurations $|\Phi_i^a\rangle$, doubly excited configurations $|\Phi_{ij}^{ab}\rangle$, etc., where $i, j, \ldots$ denotes occupied orbitals and $a, b, \ldots$ unoccupied ones. Following standard perturbation theory, the single-excitation contribution to the 2nd-order correlation energy is given by

$$\begin{aligned}
E_c^{\rm SE} &= \sum_i^{\rm occ}\sum_a^{\rm unocc}\frac{|\langle\Phi_0|\hat{H}'|\Phi_i^a\rangle|^2}{|E_0^{(0)}-E_{i,a}^{(0)}|} \\
&= \sum_i^{\rm occ}\sum_a^{\rm unocc}\frac{|\langle\Phi_0|\sum_{i<j}^{N}\frac{1}{|\mathbf{r}_i-\mathbf{r}_j|} - \sum_{i=1}^{N}v_i^{\rm MF}|\Phi_i^a\rangle|^2}{|\epsilon_i-\epsilon_a|}
\end{aligned} \tag{2}$$

where we have used the fact $E_0^{(0)} - E_{i,a}^{(0)} = \epsilon_i - \epsilon_a$.

To proceed, the numerator of Eq. (2) needs to be evaluated. This can most easily be done using second-quantization

$$\begin{aligned}
\sum_{i<j}^{N}\frac{1}{|\mathbf{r}_i-\mathbf{r}_j|} &\rightarrow \frac{1}{2}\sum_{pqrs}\langle pq|rs\rangle c_p^\dagger c_q^\dagger c_s c_r, \\
\sum_{i=1}^{N} v_i^{\rm MF} &\rightarrow \sum_{pq}\langle p|v^{\rm MF}|q\rangle c_p^\dagger c_q,
\end{aligned}$$

where p, q, r, s are arbitrary spin-orbitals from Eq. (1), $c_p^\dagger$ and c_q, etc. are the electron creation and annihilation operators, and $\langle pq|rs\rangle$ the two-electron Coulomb integrals

$$\langle pq|rs\rangle = \int d\mathbf{r}d\mathbf{r}'\frac{\psi_p^*(\mathbf{r})\psi_r(\mathbf{r})\psi_q^*(\mathbf{r}')\psi_s(\mathbf{r}')}{|\mathbf{r}-\mathbf{r}'|}.$$

The expectation value of the two-particle Coulomb operator between the ground-state configuration Φ_0 and the single excitation Φ_i^a is given by

$$\begin{aligned}
\langle\Phi_0|\frac{1}{2}\sum_{pqrs}\langle pq|rs\rangle c_p^\dagger c_q^\dagger c_s c_r|\Phi_i^a\rangle &= \sum_p^{\rm occ}\left[\langle ip|ap\rangle - \langle ip|pa\rangle\right] \\
&= \langle\psi_i|v^{\rm HF}|\psi_a\rangle
\end{aligned} \tag{3}$$

where $v^{\rm HF}$ is the HF single-particle potential.

The expectation value of the mean-field single-particle operator $v^{\rm MF}$, on the other hand, is given by

$$\begin{aligned}
&\langle\Phi_0|\sum_{pq}\langle p|v^{\rm MF}|q\rangle c_p^\dagger c_q|\Phi_i^a\rangle = \langle\psi_i|v^{\rm MF}|\psi_a\rangle \\
&= -\langle\psi_i| - \frac{1}{2}\nabla^2 + \hat{v}_{\rm ext}|\psi_a\rangle.
\end{aligned} \tag{4}$$

To arrive at Eq. (4), we have used the fact that the ψ's are eigenstates of $\hat{h}^0 = -\frac{1}{2}\nabla^2 + v_{\rm ext} + v^{\rm MF}$, and hence all non-diagonal elements $\langle\psi_i|\hat{h}^0|\psi_a\rangle$ are zero. Combining Eqs. (2), (3), and (4), yields

$$\begin{aligned}
E_c^{\rm SE} &= \sum_i^{\rm occ}\sum_a^{\rm unocc}\frac{|\langle\psi_i| - \frac{1}{2}\nabla^2 + \hat{v}_{\rm ext} + \hat{v}^{\rm HF}|\psi_a\rangle|^2}{|\epsilon_i-\epsilon_a|} \\
&= \sum_i^{\rm occ}\sum_a^{\rm unocc}\frac{|\langle\psi_i|\hat{f}|\psi_a\rangle|^2}{|\epsilon_i-\epsilon_a|}
\end{aligned}$$

where $\hat{f}$ is the single-particle HF Hamiltonian, or simply Fock operator.

For the HF reference state, i.e., when $v^{\rm MF} = v^{\rm HF}$, the ψ's are eigenstates of the Fock operator, and hence Eq. (2) is zero. For any other reference state, e.g., the KS reference state, the ψ's are no longer eigenstates of the Fock operator, and Eq. (2) is in general not zero. This gives rise to a finite single-excitation contribution to the second-order correlation energy.